Veterinary Medicine and Science

WILEY

CASE REPORT OPEN ACCESS

Dogs

Feasibility of ^{18}F-Fluorodeoxyglucose Positron Emission Tomography/Computed Tomography for the Assessment of Canine Granulosa Cell Tumours in Two Dogs

Seungwook Kim[1] | Jinyoung Choi[1] | Yujin Kim[1] | Yeon Chae[2] | Hakhyun Kim[2] | Byeong-Teck Kang[2] | Min Jang[3] | Sungin Lee[1]

[1]Department of Veterinary Surgery, College of Veterinary Medicine, Chungbuk National University, Cheongju, Republic of Korea | [2]Laboratory of Veterinary Internal Medicine, College of Veterinary Medicine, Chungbuk National University, Cheongju, Republic of Korea | [3]Department of Veterinary Surgery, College of Veterinary Medicine, Kyungpook National University, Daegu, Republic of Korea

Correspondence: Sungin Lee (sunginlee@cbnu.ac.kr)

Received: 15 February 2024 | **Revised:** 26 June 2024 | **Accepted:** 1 November 2024

Funding: This work was supported by "Regional Innovation Strategy (RIS)" through the National Research Foundation (NRF) of Korea funded by the Ministry of Education (MOE) (2021RIS-001) and also supported by the Basic Research Lab Program (2022R1A4A1025557) through the National Research Foundation (NRF) of Korea, funded by the Ministry of Science and ICT.

Keywords: ^{18}F-2-deoxy-2-fluoro-D-glucose positron emission tomography/computed tomography | canine | case report | granulosa cell tumour | ovarian tumour

ABSTRACT

Two spayed female mongrels were presented for an abdominal mass and metastasis examination. To investigate suspected ovarian tumours and metastasis, ^{18}F-2-deoxy-2-fluoro-D-glucose (^{18}F-FDG) positron emission tomography (PET)/computed tomography (CT) was performed. ^{18}F-FDG PET revealed mildly increased glucose uptake (maximum standardised uptake values, 2.03 and 1.32) without hypermetabolic invasion to adjacent tissue or lymphadenopathy. Histopathological examination confirmed that the excised ovarian tumours were granulosa cell tumours without angiolymphatic invasion. This is the first case report describing the feasibility of using ^{18}F-FDG PET/CT to detect canine granulosa cell tumours, highlighting their characteristics and identifying metastasis to regional lymph nodes or visceral organs.

1 | Introduction

Canine ovarian tumours include epithelial, sex cord-stromal and germ cell tumours and are rare neoplasms with an overall malignancy rate of 64% (Patnaik and Greenlee 1987). Granulosa cell tumours (GCTs) are the most common type of sex cord-stromal tumours, characterised by being unilateral, firm, cystic, haemorrhagic and necrotising (Diez-Bru et al. 1998). Ovarian cancer in dogs presents with non-specific clinical symptoms, such as abdominal distention, abnormal oestrus, vaginal discharge and lethargy, which may pose a challenge in diagnosis. Abdominal radiography and ultrasonography are used to determine the location of ovarian tumours and detect metastasis at other sites. Ovarian tumours can be distinguished based on their cytological and histopathological findings. Surgical resection is the recommended treatment for ovarian tumours with no metastatic evidence. In cases with metastasis, adjuvant radiotherapy and chemotherapy may be considered potential treatment options (Diez-Bru et al. 1998).

^{18}F-2-deoxy-2-fluoro-D-glucose (^{18}F-FDG) positron emission tomography (PET)/computed tomography (CT) is an imaging technique that combines both anatomical and functional imaging using radioisotopes (Bailey et al. 2005). By merging physiological and anatomical data from PET and CT, respectively, this approach allows for early tumour localisation before anatomical

changes, detection of metastasis to regional lymph nodes or distant organs, monitoring of disease recurrence and assessment of post-treatment response. ^{18}F-FDG, which is a commonly used radiotracer, exhibits increased glucose uptake that is visualised as intense signals on PET images. This property enables the identification of hypermetabolic conditions typical of tumours and inflammation. Glucose uptake is measured using the standardised uptake value (SUV), which is calculated as the average tissue concentration of ^{18}F-FDG (MBq/mL) divided by the injected dose (MBq) per body weight (g) (Lucignani, Paganelli, and Bombardieri 2004). SUV, which represents the ratio of the concentration of radioactivity in a region of interest to that of the entire body, indicates tissue metabolic activity. In human medicine, ^{18}F-FDG PET/CT has proven to be a valuable diagnostic tool for distinguishing malignant ovarian tumours and detecting metastasis. In a study, ^{18}F-FDG PET/CT accurately identified 28 of 32 primary ovarian lesions as malignant, with SUVmax values ranging from 3.1 to 25.7 (Castellucci et al. 2007).

This case report describes the use of ^{18}F-FDG PET/CT to diagnose and evaluate canine ovarian cancer. It presents the clinical significance and potential limitations of ^{18}F-FDG PET/CT in diagnosing canine ovarian cancers, particularly GCTs.

2 | Case Presentation

2.1 | Case 1

An 11-year-old spayed female mongrel weighing 3.81 kg was presented for an abdominal mass. The patient had previously undergone an ovariohysterectomy at 6 months of age. Despite previous ovariohysterectomy, continued menstruation was observed, resulting in the discovery of an ovarian remnant on abdominal ultrasonography conducted at the age of 2 years. An abdominal mass was detected on radiography during a regular medical examination 3 months prior to presentation. The patient was referred to our hospital for abdominal mass resection.

Physical examination revealed normal vital signs (heart rate, 144 bpm; respiratory rate, 24 bpm; systolic blood pressure, 120 mmHg; body temperature, 38.3°C); however, a grade 3/6 systolic murmur was auscultated at the left apex. The patient was diagnosed with American College of Veterinary Internal Medicine stage B1 myxomatous mitral valve disease based on echocardiography findings. Complete blood count, serum chemistry and blood gas analysis revealed no significant abnormalities except for mild thrombocytosis (556×10^3/μL; reference range, $148–484 \times 10^3$/μL) and increased alkaline phosphatase levels (808 IU/L; reference range, 29–97 IU/L). Radiographic examination revealed an irregular oval mass (75 × 46 mm) at the L1–L6 levels and abdominal ultrasonography showed a fluid-filled tubular mass (65.9 × 37.3 mm) with multiple cystic lesions located caudally to the right kidney.

2.2 | Case 2

A 9-year-old spayed female mongrel weighing 11.32 kg was referred for metastasis examination after tumour resection. The patient had undergone an ovariohysterectomy at 12 months of age. However, an ovarian remnant was found at the age of 2 years on abdominal ultrasonography. Masses were observed on the left fifth mammary gland and left metatarsal region, for which a simple mastectomy and skin mass resection were performed 1 month prior to presentation. Based on histopathological examination, the masses were diagnosed as mammary gland adenoma and cutaneous soft tissue sarcoma.

Physical examination revealed normal vital signs (heart rate, 128 bpm; respiratory rate, 24 bpm; systolic blood pressure, 132 mmHg; body temperature, 38.1°C). Results of complete blood count, serum chemistry and blood gas analysis were within the reference range, except for increased alkaline phosphatase (215 IU/L; reference range, 29–97 IU/L) and alanine aminotransferase (188 IU/L; reference range, 21–102 IU/L). Radiography and ultrasonography did not reveal any significant findings or metastatic evidence, except for a suspected ovarian remnant on abdominal ultrasound.

2.3 | CT and PET

CT and PET were performed to assess potential metastasis and recurrence. The patients had to fast for 12 h before anaesthesia induction. General anaesthesia was induced using intravenous propofol (6 mg/kg; Freefol-MCT, Daewon Pharm. Co., Ltd.; Seoul, South Korea) and midazolam (0.2 mg/kg; Midazolam, Bukwang Pharm. Co. Ltd.; Seoul, South Korea), followed by a maintenance dose with 2.0% isoflurane inhalation (Terrell; Piramal Critical Care; Bethlehem, PA, USA) and 100% oxygen ventilation. The patients were positioned in sternal recumbency throughout PET/CT. ^{18}F-FDG intravenous injection (0.64 and 1.92 mCi in cases 1 and 2, respectively) was administered during anaesthesia induction. Heart rate, respiratory rate, systolic blood pressure, body temperature, percutaneous oxygen saturation, end-tidal CO_2 concentration and minute ventilation volume were monitored during anaesthesia. A 20-min full-body CT was performed using a four-row multidetector CT scanner at 100 mAs and 120 kVp, with a slice thickness of 1.25 mm. Post-contrast images were obtained using intravenous iohexol (880 mg/kg; Omnipaque; GE Healthcare Co., Ltd.; Marlborough, MA, USA). In case 1, CT revealed increased opacity in the suspected right ovarian tumour (52.9 × 43.4 × 71.0 mm) (Figure 1A), with contrast enhancement observed along the margin (Figure 1B). In case 2, CT highlighted the suspected left ovarian tumour (12.4 × 10.3 × 10.9 mm) caudolateral to the left kidney (Figure 1E,F). Subsequently, PET (Discovery-72 STE, General Electric Medical Systems; Waukesha, WI, USA) was conducted 60 min after the administration of ^{18}F-FDG, and the PET image was analysed using the RadiAnt DICOM Viewer. Regions of interest were manually delineated on PET/CT fusion images. The SUV of both suspected ovarian tumours indicated a slight increase in glucose uptake (SUVmax, 2.03 and 1.32 for cases 1 and 2, respectively) (Figure 1C,G). Specifically, the suspected ovarian mass in case 1 showed a mild increase along the periphery, corresponding to the regions of contrast enhancement (Figure 1C). The PET/CT scan of case 1 did not reveal glucose uptake in the centre of the mass (SUVmax, 0.1787; SUVmean, 0.1033). Both cases did not delineate any hypermetabolic invasion of adjacent structures or lymphadenopathy (Figure 1D,H).

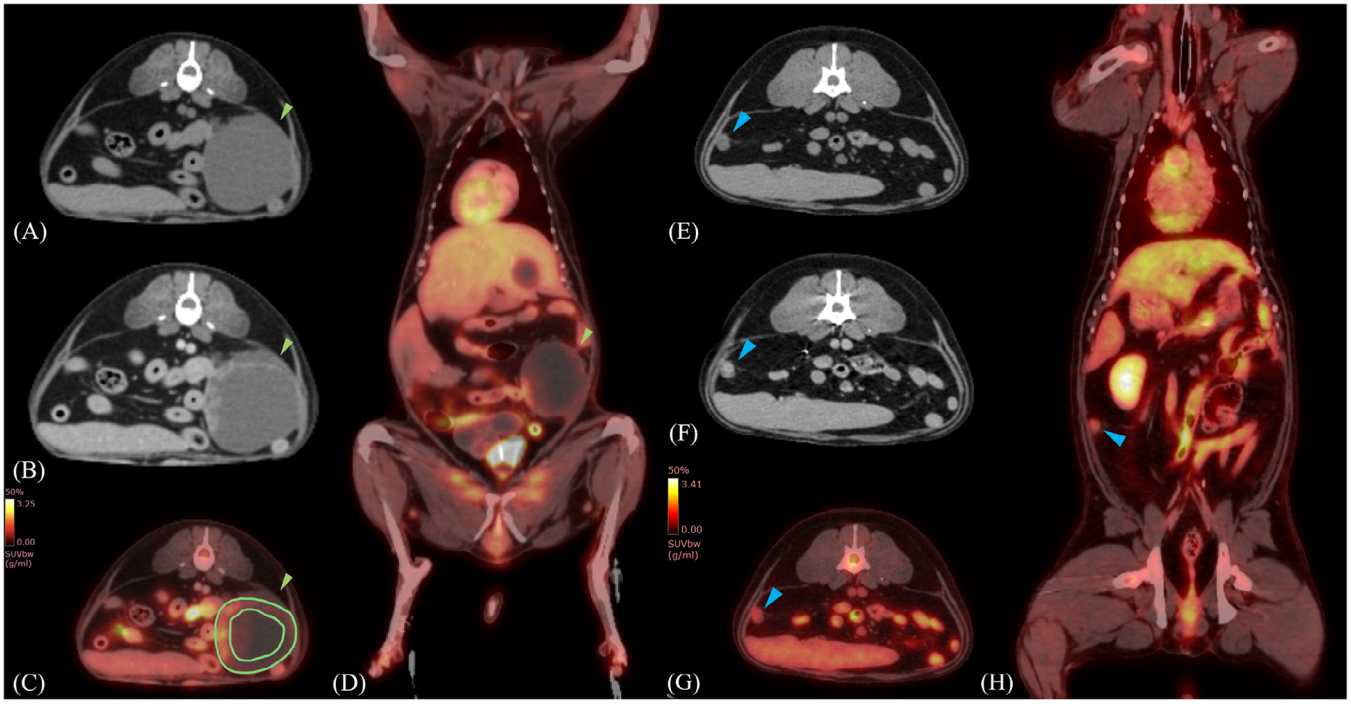

FIGURE 1 | Pre- and post-contrast CT and fused PET/CT images using ^{18}F-FDG as contrast in two dogs with granulosa cell tumours. (A) In case 1, axial plane CT reveals a mass (green arrowhead) (52.9 × 43.4 × 71.0 mm) caudal to the right kidney and (B) contrast enhancement along the periphery of the lesion on the post-contrast CT images. (C) In case 1, SUVs of ^{18}F-FDG PET/CT fusion images highlight the mild increase in glucose uptake on the border (SUVmax, 2.03) without elevation of glucose uptake at the centre (SUVmax: 0.1787; SUVmean: 0.1033). (D) In case 1, coronal plane PET/CT reveals the absence of hypermetabolic activity in the adjacent organs or lymph nodes. In case 2, axial plane (E) pre- and (F) post-contrast CT images illustrate the lesion (blue arrowhead) (12.4 × 10.3 × 10.9 mm) positioned caudolateral to the left kidney. (G) In case 2, the fused ^{18}F-FDG PET/CT images indicate a low FDG-avid nature of the mass (SUVmax, 1.32; SUVmean, 1.11). (H) In case 2, coronal plane PET/CT reveals no FDG uptake elevation in the lymph nodes or visceral organs. ^{18}F-FDG PET/CT, ^{18}F-fluorodeoxyglucose positron emission tomography computed tomography; SUV, standardised uptake value.

2.4 | Surgical Procedure and Postoperative Course

The abdominal masses were surgically resected to prevent potential rupture and evaluate histopathologic findings. In case 1, pimobendan (0.25 mg/kg; Vetmedin; Boehringer Ingelheim Promeco; S.A. de C. V., Mexico) was administered orally for a month before surgery to lower the risk of complications from heart disease. Intravenous propofol (5 mg/kg) and midazolam (0.2 mg/kg) were injected for anaesthesia induction. Under general anaesthesia using 2.0% isoflurane with 100% oxygen ventilation and intravenous infusion of Hartmann's solution (1.5 mL/kg/h), an exploratory laparotomy was performed to examine the origin of the lesions and for tumour resection. The ovarian tumours caudal to the right and left kidney in cases 1 and 2, respectively, were excised by resecting the suspensory ligament and ovarian pedicle (Figure 2A,B). The surgeries proceeded without any complications, and postoperative recoveries were uneventful. Remifentanil (2.5 μg/kg/h; Tivare; BCWORLD Pharm. Co., Ltd.; Yeojoo, South Korea) was injected intravenously for pain management during and after surgery. The patients were discharged 3 days after surgery and followed up for 3 months. Radiography and ultrasonography findings showed no evidence of recurrence or metastasis in both cases.

The resected tumours were immediately fixed in 10% formaldehyde and sent for histopathological analysis the following day (IDEXX Laboratories, Inc., USA). The neoplasms in both cases were diagnosed as GCTs, and angiolymphatic invasion was not observed on histopathological examination in either case (Figure 3).

3 | Discussion

This case report highlights the use of ^{18}F-FDG PET/CT to characterise ovarian tumours and identify metastatic lymph nodes and organs. ^{18}F-FDG PET/CT provides supplementary information on ovarian cancer in addition to the radiographic and ultrasound findings. It exhibits superior efficacy compared to CT alone in terms of staging (accuracy: 92.1%), thereby enabling surveillance of recurrence and facilitating adjustments in the treatment plans (Nam et al. 2010; Simcock et al. 2006). ^{18}F-FDG PET/CT application in veterinary medicine is currently limited, particularly for the diagnosis and staging of certain tumour types (Kim et al. 2014; Lee et al. 2022; Kim and Lee 2023). This case report demonstrates the feasibility of using ^{18}F-FDG PET/CT to characterise and identify metastasis of canine GCTs.

SUVmax above 2.5 is generally recognised as an indication of malignancy, and SUVmax of 3.0 is considered the threshold for human ovarian malignancy (sensitivity: 87%; specificity: 100%) (Castellucci et al. 2007). Choi et al. reported SUVmax and

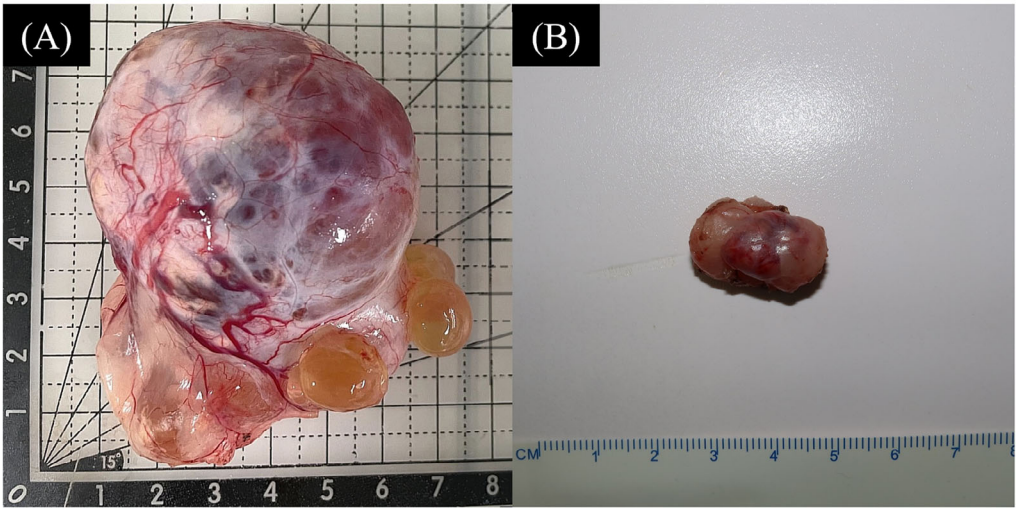

FIGURE 2 | Gross pathology of the resected ovarian tumours in two dogs with granulosa cell tumours. (A) The mass (55 × 68 mm) in case 1 is encapsulated with a lobulated smooth surface with multiple cystic and haemorrhagic areas. (B) The tumour (12.4 × 10.8 mm) in case 2 appears as a firm mass surrounded by adipose tissues.

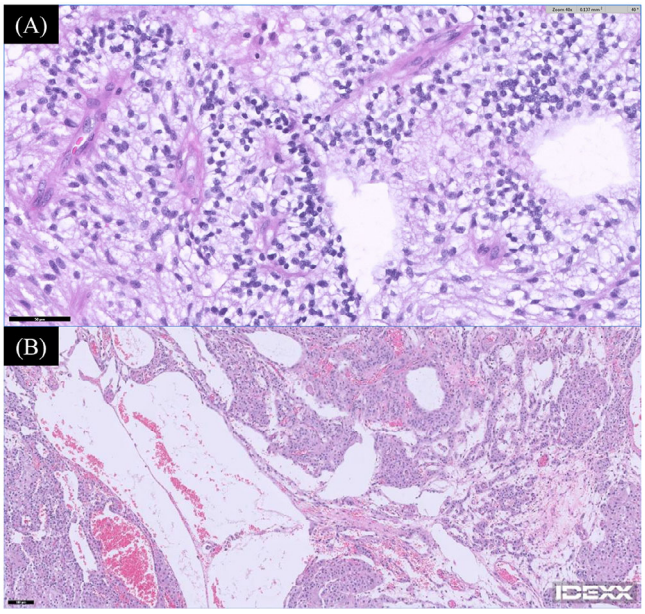

FIGURE 3 | Histopathology of two canine granulosa cell tumours. (A) The normal ovarian architecture is infiltrated and substituted by a multinodular mass of densely packed, moderately pleomorphic neoplastic epithelial cells with indistinct margins. The mass is diagnosed as a granulosa cell tumour with a mitotic count of two per 2.37 mm^2. The angiolymphatic invasion was not observed. (B) The ovarian structure is obscured by a noticeably defined, expanding and infiltrating tumour composed of irregularly shaped tubules with varying sizes and luminal spaces. The tumour is diagnosed as a granulosa cell tumour. The mitotic count was six per 2.37 mm^2. No evidence of invasion into blood or lymphatic vessels was found.

SUVmean values of 1.45 ± 0.22 and 1.19 ± 0.16, respectively, for normal canine ovaries (Lee et al. 2024). GCTs are malignant ovarian tumours with a metastasis rate of approximately 20%, and they usually invade to sublumbar lymph nodes, liver, pancreas and lungs (Patnaik and Greenlee 1987). In both cases, the lesions exhibited SUVmax below 3.0, illustrating low ^{18}F-FDG avidity of GCTs. Notably, the glucose uptake in case 2 falls within the normal reference range. Likewise, human GCTs exhibit SUVmax of 2.4 ± 0.9, indicating lower glucose uptake than other ovarian cancers (SUVmax, 7.6; SUVmean, 4.5) (Roze et al. 2021; Park et al. 2015). False-negative findings have been observed on PET/CT, particularly in cystic or mucinous tumours demonstrating a distinctly low metabolic rate in the centre of the cyst or tumour wall (Kawahara et al. 2004). Similarly, the lesion in case 1 exhibited a uniquely low SUV in the centre and only a slight increase in SUV along the periphery, which was attributed to its cystic nature.

One of the major prognostic factors for canine GCTs is the presence of metastasis. In the field of canine ovarian oncology, the mean survival time for early GCTs is significantly longer than that for advanced GCTs (≤ T2: 1474 days vs. ≥ T3: 443 days; $p = 0.002$), and the presence of metastatic disease indicates a poor prognosis (present: 391 days vs. absent: 1474 days; $p < 0.001$) (Goto et al. 2021). In human medicine, PET/CT has demonstrated high sensitivity (73.2%) and specificity (96.7%) in detecting metastatic lymph nodes and distant metastases compared with that of CT (sensitivity: 42.6%; specificity: 95.0%) and magnetic resonance imaging (sensitivity: 54.7%; specificity: 88.3%) (Yuan et al. 2012). In this case report, post-operative radiography and ultrasound demonstrated no metastasis. No ^{18}F-FDG-avid lesions were identified in the regional lymph nodes or organs, and no angiolymphatic invasion was identified on histopathological examination, suggesting the absence of metastasis.

A limitation of this case report is the need for further studies with larger populations to establish statistical significance. In both cases, metastasis was not examined at the time of the PET scan or during the follow-up period. Consequently, further research is required to confirm the efficacy of ^{18}F-FDG PET/CT in detecting metastasis. PET/CT is routinely conducted in human ovarian cancer to investigate potential metastasis, recurrence and therapeutic response. In this case, we were unable to perform repeated PET/CT scans to assess systemic metastasis and disease recurrence because of the owners' compliance.

To the best of our knowledge, this is the first case report demonstrating the utility of PET/CT for canine GCTs. GCTs exhibited a distinctively low ^{18}F-FDG uptake compared to other canine malignancies. Given the high malignancy rate observed in canine ovarian tumours, including GCTs, the possibility of ovarian malignancy should not be ruled out, and surgical resection is recommended despite observing low metabolic activity. Moreover, the cases underscore the role of PET/CT in detecting metastasis. This case report provides diagnostic insights and highlights the potential shortcomings of PET/CT, thus establishing fundamental knowledge regarding canine GCTs.

Author Contributions

Sungin Lee: conceptualisation, funding acquisition, investigation, methodology, project administration, supervision, validation, writing–original draft, writing–review and editing. **Seungwook Kim**: conceptualisation, formal analysis, investigation, methodology, software, visualisation, writing–original draft, writing–review and editing. **Jinyoung Choi**: data curation, formal analysis, software, writing–review and editing. **Yujin Kim**: formal analysis, visualisation, writing–review and editing. **Yeon Chae**: data curation, resources, software, writing–review and editing. **Hakhyun Kim**: data curation, project administration, resources, writing–review and editing. **Byeong-Teck Kang**: data curation, project administration, resources, writing–review and editing. **Min Jang**: data curation, project administration, validation, writing–review and editing.

Acknowledgements

The authors would like to thank the owners of the dogs for consenting to publish this report.

Ethics Statement

Ethical review and approval were not required for the animal study because this is the case report of a clinical patient, not an experimental research paper on animals. Written informed consent was obtained from the owners for the participation of their animals in this study. Written informed consent was obtained from the owner of the patient for the publication of this case report. The authors would like to extend their appreciation for this consent.

Conflicts of Interest

The authors declare no conflicts of interest.

Data Availability Statement

The data that support the findings of this study are available on request from the corresponding author. The data are not publicly available due to privacy or ethical restrictions.

Peer Review

The peer review history for this article is available at https://publons.com/publon/10.1002/vms3.70126.

References

Bailey, D. L., M. N. Maisey, D. W. Townsend, and P. E. Valk eds. 2005. *Positron Emission Tomography*, Vol. 2, p. 22. London, UK: Springer.

Castellucci, P., A. M. Perrone, M. Picchio, et al. 2007. "Diagnostic Accuracy of 18F-FDG PET/CT in Characterizing Ovarian Lesions and Staging Ovarian Cancer: Correlation With Transvaginal Ultrasonography, Computed Tomography, and Histology." *Nuclear Medicine Communications* 28, no. 8: 589–595. https://doi.org/10.1097/MNM.0b013e3281afa256.

Diez-Bru, N., I. Garcia-Real, E. M. Martinez, E. Rollan, A. Mayenco, and P. Llorens. 1998. "Ultrasonographic Appearance of Ovarian Tumors in 10 Dogs." *Veterinary Radiology & Ultrasound* 39, no. 3: 226–233. https://doi.org/10.1111/j.1740-8261.1998.tb00345.x.

Goto, S., R. Iwasaki, H. Sakai, and T. Mori. 2021. "A Retrospective Analysis on the Outcome of 18 Dogs With Malignant Ovarian Tumours." *Veterinary and Comparative Oncology* 19, no. 3: 442–450. https://doi.org/10.1111/vco.12639.

Kawahara, K., Y. Yoshida, T. Kurokawa, et al. 2004. "Evaluation of Positron Emission Tomography With Tracer 18-Fluorodeoxyglucose in Addition to Magnetic Resonance Imaging in the Diagnosis of Ovarian Cancer in Selected Women After Ultrasonography." *Journal of Computer Assisted Tomography* 28, no. 4: 505–516. https://doi.org/10.1097/00004728-200407000-00011.

Kim, J., S. Y. Kwon, R. Cena, et al. 2014. "CT and PET-CT of a Dog With Multiple Pulmonary Adenocarcinoma." *Journal of Veterinary Medical Science* 76, no. 4: 615–620. https://doi.org/10.1292/jvms.13-0434.

Kim, S. H., and S. Lee. 2023. "Case Report: 18F-2-deoxy-2-fluoro-D-glucose Positron Emission Tomography/Computed Tomography Image Findings of a Dog With Gossypiboma." *Frontiers in Veterinary Science* 10: 1107238. https://doi.org/10.3389/fvets.2023.1107238.

Lee, D., T. Yun, Y. Koo, et al. 2022. "18F-FDG PET/CT Image Findings of a Dog With Adrenocortical Carcinoma." *BMC Veterinary Research* 18, no. 1: 1–7. https://doi.org/10.1186/s12917-021-03102-6.

Lee, S., J. Choi, Y. Chae, and B. Kang. 2024. "Physiological Ranges of 18 F-fluoro-2-deoxy-D-glucose Uptake in Normal Ovaries of Dogs From Positron Emission Tomography/Computed Tomography." *Frontiers in Veterinary Science* 11: 1343695. https://doi.org/10.3389/fvets.2024.1343695.

Lucignani, G., G. Paganelli, and E. Bombardieri. 2004. "The Use of Standardized Uptake Values for Assessing FDG Uptake With PET in Oncology: A Clinical Perspective." *Nuclear Medicine Communications* 25, no. 7: 651–656. https://doi.org/10.1097/01.mnm.0000134329.30912.49.

Nam, E. J., M. J. Yun, Y. T. Oh, et al. 2010. "Diagnosis and Staging of Primary Ovarian Cancer: Correlation Between PET/CT, Doppler US, and CT or MRI." *Gynecologic Oncology* 116, no. 3: 389–394. https://doi.org/10.1016/j.ygyno.2009.10.059.

Park, T., S. Lee, S. Park, et al. 2015. "Value of 18 F-FDG PET/CT in the Detection of Ovarian Malignancy." *Nuclear Medicine and Molecular Imaging* 49: 42–51. https://doi.org/10.1007/s13139-014-0303-3.

Patnaik, A. K., and P. G. Greenlee. 1987. "Canine Ovarian Neoplasms: A Clinicopathologic Study of 71 Cases, Including Histology of 12 Granulosa Cell Tumors." *Veterinary Pathology* 24, no. 6: 509–514. https://doi.org/10.1177/030098588702400607.

Roze, J. F., H. S. van Meurs, G. R. Monroe, et al. 2021. "[18F] FDG and [18F] FES Positron Emission Tomography for Disease Monitoring and Assessment of Anti-Hormonal Treatment Eligibility in Granulosa Cell Tumors of the Ovary." *Oncotarget* 12, no. 7: 665. doi: 10.18632/oncotarget.27925.

Simcock, B., D. Neesham, M. Quinn, E. Drummond, A. Milner, and R. J. Hicks. 2006. "The Impact of PET/CT in the Management of Recurrent Ovarian Cancer." *Gynecologic Oncology* 103, no. 1: 271–276. https://doi.org/10.1016/j.ygyno.2008.08.027.

Yuan, Y., Z. X. Gu, X. F. Tao, and S. Y. Liu. 2012. "Computer Tomography, Magnetic Resonance Imaging, and Positron Emission Tomography or Positron Emission Tomography/Computer Tomography for Detection of Metastatic Lymph Nodes in Patients With Ovarian Cancer: A Meta-Analysis." *European Journal of Radiology* 81, no. 5: 1002–1006. https://doi.org/10.1016/j.ejrad.2011.01.112.